

Numerical simulation of framed joints in sawn-timber roof trusses

J. R. Villar¹, M. Guaita^{*2}, P. Vidal¹ and R. Argüelles Bustillo³

¹ *Escuela de Ingenierías Agrarias. Universidad de Extremadura. Ctra. Cáceres s/n. 06071 Badajoz. Spain.*

² *Escuela Politécnica Superior. Universidad de Santiago de Compostela. C/ Benigno Ledo s/n. 27002 Lugo. Spain.*

³ *Escuela de Ingenieros de Montes. Universidad Politécnica de Madrid. Ciudad Universitaria s/n. 28040 Madrid. Spain.*

Abstract

This paper presents an analysis of carpentry joints between structural timber members based on numerical simulation. In conventional design, simplifying assumptions of the stress distribution and the transmission of forces on the contacting surfaces are made, and the effect of contact friction between surfaces is neglected. Whereas a number of authors have been concerned with other types of joints, such as mechanical or glued joints between timber members, carpentry joints have hardly been subject to numerical simulations. This study presents a more realistic approach to the behaviour of these joints, using the finite element method, which enables further knowledge of the stresses acting on the joint. In addition, the finite element method enables the optimization of the geometric definition of carpentry joints between structural timber members. The numerical simulations performed for framed joints have revealed that friction between contacting surfaces has particular relevance for the behaviour of the joint. The Spanish Technical Building Code, among others, is based on conventional design. Numerical simulations have revealed a high level of safety in such a conventional definition of framed joints.

Additional key words: connections, finite element method, orthotropic materials, structural timber.

Resumen

Simulación numérica de ensambles en barbilla en cerchas de madera aserrada

En este artículo se presenta un análisis de uniones por ensamble embarbillado entre piezas de madera estructural basado en el empleo de la simulación numérica. El cálculo convencional se realiza a través de unos supuestos simplificadores de distribución de tensiones y de transmisión de las fuerzas sobre las caras en contacto, al mismo tiempo que se desprecia el efecto del rozamiento por contacto entre ellas. Mientras que existe cierta cantidad de trabajos relacionados con otros tipos de uniones entre piezas de madera, mecánicas, encoladas, etc., las uniones carpinteras o tradicionales apenas han sido objeto de simulaciones numéricas. En este trabajo se presenta una visión más cercana a la realidad del comportamiento de estos ensambles por medio del método de los elementos finitos, lo que permite aproximarse más al conocimiento de los esfuerzos actuantes y buscar una mayor optimización en la definición geométrica de los mismos. Se aprecia en las simulaciones numéricas realizadas que, en este tipo de ensambles, la fricción entre superficies en contacto adquiere una alta importancia en el comportamiento de la unión; al mismo tiempo, el cálculo convencional en el que se basa, entre otros, el Código Técnico Español de la Edificación, deja ampliamente del lado de la seguridad la definición dimensional de estas uniones por ensamble embarbillado.

Palabras clave adicionales: madera estructural, materiales ortótropos, método de elementos finitos, uniones.

* Corresponding author: guaita@lugo.usc.es

Received: 01-12-06. Accepted: 16-10-08.

M. Guaita and P. Vidal are members of the SEA.

Introduction

The reduced costs and increased precision of computer aided manufacturing has contributed to the use of sawn timber –also termed solid timber– in traditional carpentry joints (Kessel, 1995). Traditional carpentry joints are used structurally, mainly for designing floor and roof structures for many types of buildings.

In the traditional design of roof trusses, all the intersections are assembled by framed joints. The cogging joint is particularly interesting because it is a critical point in stress transmission. The joints analysed in this study are interlocked by bevelling the members, such that the loads are transmitted through local compressions and shearing stresses, and through friction between the contacting surfaces.

Behaviour of wood at the joint

The structure of wood is characterised by the anisotropic properties of the material, which are essential for the mechanical behaviour of wood and vary according to the direction between stress and grain. Wood is an orthotropic material with different properties in three mutually orthogonal directions: axial, radial and tangential. The strength properties of wood in the axial direction or parallel to the grain are good, while smaller values are observed in the other directions.

Wood shows high bending strength. Roughly, the load capacity in bending structures-to-weight ratio of wood is 1.3 times the ratio for steel, and 10 times the ratio for concrete (Argüelles *et al.*, 2003). Conversely, wood shows a low modulus of elasticity and low compressive or tensile strength perpendicular to the grain, which is a peculiar characteristic of wood as compared to other materials. These properties particularly affect joints between timber members.

The mechanical properties of wood are dependent on quality. The mechanical properties of wood are designed based on strength criteria, in compliance with European Standard EN 338 (CEN, 2003), which defines strength classes for sawn timber.

In framed joints, loads are transmitted through local compressions and shearing stresses and through friction between the contacting surfaces. Conventional design uses a number of simplifying assumptions that affect the occurrence of friction, the acting forces and the distribution of stresses. The finite-element based analysis of

this type of joints allows for the introduction of such simplifications in the design.

In the conventional and simplified design of framed joints, the following simplifications are considered:

- Forces F_{1d} (N) and F_{2d} (N) on the surfaces of the joint act perpendicular to the surfaces on which the forces act (Fig. 1A), which means that contact friction between members is neglected, such that friction does not add to load transmission.
- An oblique compression acts on the joint, assuming that the direction of the grain is parallel to the member centre-line.
- The distribution of section forces on the contacting surfaces is based on different distribution assumptions. In some cases, it is assumed that the section corresponding to F_{1d} receives almost the entire load (Natterer *et al.*, 2000).

The Spanish Technical Building Code [Ministerio de la Vivienda, 2006; abbreviated to CTE-SE-M (2006)] has recently been approved and regulates the design of wood structures in Spain. The Code contains criteria for calculating the stresses that occur in the members of assembled joints and the geometric constraints – notch depth t (mm) and chord shear length a (mm) – that these joints must satisfy for structural stability (Fig. 1A). Such criteria are explained below, as taken from CTE-SE-M (2006). The verification procedure has been taken from the Swiss draft standard for timber structures (SIA, 2002).

The oblique compression strength at the oblique intersection between members derives from the Hankinson formula, included in CTE-SE-M (2006):

$$f_{c,\alpha,d} = \frac{f_{c,0,d}}{\frac{f_{c,0,d}}{f_{c,90,d}} \cdot \sin^2 \alpha + \cos^2 \alpha}$$

where $f_{c,\alpha,d}$ is the design compression strength in N mm² in a direction with respect to the grain, in degrees; $f_{c,0,d}$ is the design compression strength parallel to the grain, and $f_{c,90,d}$ is the design compression strength perpendicular to the grain, which shall be constrained by multiplying the value of the strength by a factor of 0.8.

Cogging joints must satisfy the following conditions:

- Chord shear length $a \geq \frac{F_d \cos \beta}{bf_{v,d}}$
- Notch depth $t \geq \frac{F_d \cos \beta}{bf_{c,\alpha,d}}$

where: b is member width in mm, β is the angle between the force F_d in N and the direction of the grain in the

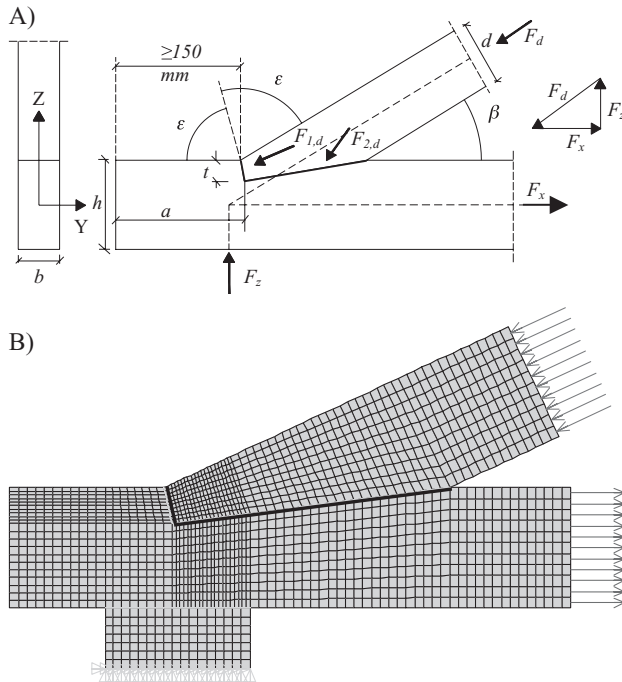


Figure 1. Free-body diagram, mesh and deformed shape. A: Cogging joint, as taken from the CTE-SE-M (2006). B: Finite element meshing of the model.

tie (Fig. 1A) in degrees; and $f_{v,d}$ is the design value of shear strength in N mm^{-2} . In addition, notch depth must meet the conditions established in Table 1.

Previous studies of interest for numerical simulation of wood truss joints

Generally, the studies concerned with timber joints have focused on mechanical fasteners. Ellegaard (2006) presented a finite-element model for the analysis of timber trusses with punched metal plate fasteners. The model included the semirigid and nonlinear behaviour of the joints. Timber beams had linear-elastic properties.

Table 1. Additional conditions established for notch depth in CTE-SE-M (2006)

Skew angle (β , degrees)	Notch depth (t , mm)
≤ 50	$t \leq h/4^1$
$50 < \beta < 60$	Linearly interpolated
≥ 60	$t \leq h/6$

¹ h : tie depth in mm.

Hussein (2000) reported the numerical simulation of a metal-plate-connected joint. The author was not concerned with the transmission of stresses between truss members, but with the buckling of metal plate connectors in timber trusses.

Other authors studied the behaviour of dowel-type joints by using finite elements. Chen *et al.* (2003) presented the numerical simulation of the performance of a dowel-type joint. The model presented a wood section with a perpendicular dowel laid across a hole and was simulated considering linear orthotropy for timber and isotropy for steel. Spring elements were used for the contact.

Moses and Prion (2003) and Sawata and Yasumura (2003) studied bolted or dowel-type joints, while Williams *et al.* (2000) suggested a finite element based failure model for bolted joints.

Stehn and Börjes (2004) analysed the influence of ductility on the load-carrying capacity of glued laminated timber truss structures. Based on previous tests, the authors compared the results with a numerical model under conditions of plane stress and considering linear orthotropy for timber and isotropy for steel plates.

Parisi and Piazza (2002) analysed the behaviour of reinforced traditional timber joints subjected to cyclic loads in a truss with a span of 13 m. After having obtained the load displacement relationship, the authors modelled semirigid joints with beam elements connected by spring elements whose spring coefficients had been previously estimated.

Kharouf *et al.* (2003) modelled a bolted joint. The material was considered elastoplastic, and a simple two-dimensional plasticity model was followed for plastic behaviour.

Some authors compared numerical Finite Element Method (FEM) models and experimental models for the analysis of metal-plate-connected wood truss joints (Gupta and Gebremedhin, 1990; Vatovec *et al.*, 1996a). These authors modelled trusses with beam elements and semirigid joints, but not traditional joints (Gupta and Gebremedhin, 1992; Gupta *et al.*, 1992; Vatovec *et al.*, 1996b, 1997). However, because these authors did not analyse force transmission in wood truss traditional joints, the interest of their studies is only partial for the analysis conducted here.

Lusambo and Wills (2002) did not use numerical models, but they conducted an experimental study on round timber truss joints using frames specially designed for the joints studied. These authors used a device for measuring the applied loads and the resulting deflection, and analysed the ratio between design loads and

failure loads for the joint. However, these tests did not analyse the complete truss or the stress distribution at the joints.

Objectives

The lack of studies concerned with the analysis of the behaviour of traditional joints suggests the need to further study this type of joint, particularly because the numerical control used in the production of timber members has recently increased the use of traditional carpentry joints.

The FEM analysis of traditional joints performed in this study is aimed at observing the performance conditions of the joint in terms of the stresses that occur in the members. In addition, the study aims: 1) to quantify and characterize the forces acting on each surface of the joint and 2) to determine the influence of the section forces acting on the joint on the geometric definition of the joints studied.

Material and methods

Trusses and joints studied

This study analysed cogging joints in timber trusses. Such an analysis required performing a geometric modelling of the joint with finite elements, and introducing the values of the forces acting on the joint.

The analysis was developed (1) by using complete trusses structurally designed based on span and geometry, which enabled us to know the forces transmitted to the joints, and (2) by varying directly the intrinsic parameters of the joint related to the geometry of the joint and the forces acting on it.

The starting point of the analysis was the study and design of trusses composed of kingpost, rafters, struts and tie, a widely used conventional truss type, considering different spans and roof slopes. The design was performed using Estrumad software (vers. 2006; Argüelles Alvarez *et al.*, 2006) for matrix computations of timber structures, which allowed for the optimisation of sections and the obtention of the resulting stresses in the truss members. Truss design was performed in compliance with the European Standard EN 1995-1-1 Eurocode 5 (CEN, 2004a).

From this analysis, a set of designed real trusses was obtained, the geometric characteristics of the trusses were fully defined, and the value of the stresses that occurred in the members was determined. For the cogging joint, the following factors were considered: size of the intersecting members, angle between the members, and value of the axial forces acting on the node, compression force in the rafter and tension force in the tie.

For the analysed trusses, spans ranged 8 to 12 m, and the values of the angle between rafter and tie were 25, 30, 35, 40 and 45 degrees, which corresponded to the slope of the roof. The analysis was performed for service class 1, which corresponds to an average moisture content in most softwoods not exceeding 12%. Closed roof structures generally belong to service class 1 (Argüelles *et al.*, 2003). Timber strength classes C18 and C27 (see Table 2) were considered in the study, following the European Standard EN 338 (CEN, 2003) and the European Standard EN1912 (CEN, 2004b). The strength classes considered correspond to classes ME-2 and ME-1, respectively, according to Classification Standard UNE 56544 for Scots pine (*Pinus sylvestris* L.) of Spanish origin.

Because the analysis attempted to study a wide range of geometric variables and loads at the joint, the joints were studied isolated by varying parameters such as axial force acting on the joint, friction coefficient, skew angle, etc.

Table 2. Stiffness properties of the material for the strength classes considered

	Strength C18	Class C27
Mean modulus of elasticity parallel to the grain $E_{0, mean}$, N mm ⁻²	9000	12000
Mean modulus of elasticity perpendicular to the grain $E_{90, mean}$, N mm ⁻²	300	400
Mean shear modulus G , N mm ⁻²	560	750
Poisson's ratio ν	0.025	0.025
Characteristic density ρ_k , kg m ⁻³	320	370
Mean density ρ_{mean} , kg m ⁻³	380	450

Finite-element modelling

The finite element models developed in this study allowed for a detailed analysis of the strain-stress state in traditional framed joints. The developed model was automated and admitted variations in depths, geometries, angles between members, constraints on motion and forces acting at the node level.

In order to perform the numerical simulation of the joint, each joint was modelled in the Ansys finite element software (ANSYS, 2003), considering the corresponding geometry and loads, as described in the preceding section. The notch depth and the chord shear length were initially defined according to CTE-SE-M (2006) because the current European Standard EN 1995-1-1 Eurocode 5 (CEN, 2004a) does not include any recommendation for the type of joint studied.

A two dimensional (2D) plane stress analysis was performed, considering that thickness equalled section width. The model was developed with 'Plane42' finite elements from the Ansys element library. Plane42 can be used as a plane element (plane stress), defined by four nodes having two degrees of freedom at each node: translation in the nodal X and Y directions. In order to minimise the error, the mesh was as uniform as possible and was denser in the zones with the largest stress gradient (Fig. 1B).

A 2D elastic orthotropic model of the behaviour of the material was considered for all the elements. In the design of timber structures and in this study, the values assumed for the physical properties perpendicular to the grain comprise the radial and tangential directions because: (1) differences between both directions are small as compared to the axial direction and (2) both directions are often not recognizable in members used in timber construction. Table 2 shows the properties of the material for the strength classes considered.

The model simulated contact between surfaces. The static friction coefficient μ between the surfaces of the contacting members was assumed to have values in the range 0.60 (value for dry timber) to 0.83 (green timber) (USDA, 1974). The method used in the analysis is described below.

Groups of two different lines were defined in the contact zone established. Each of the lines belonged to a different solid but had the same coordinates and geometric position, such that the nodes of each line coincided.

To define the surface-to-surface contact (represented by a line in plane stress), the lines of friction between rafter and tie were meshed with one-dimensional con-

tact elements in the direction of the lines. The surface-to-surface contact was defined by two elements (the 'target' element and the 'contact' element) that were always associated and defined this contact pair.

Target 169 and Contact 172 elements were used, as in Vidal *et al.* (2005). These surface-to-surface contact elements were defined by two nodes for generating friction between four-node rectangular elements (in this case, Plane 42).

In the analysis, the resolution algorithm used for the contact was the augmented Lagrange method (ALM) described by Simo and Laursen (1992). After comparing the results obtained with the penalty method (PM), ALM was chosen for the calculations because this method is an iterative series of penalty methods, and its results are less sensitive to contact stiffness.

After having modelled the joint using the finite element method, the state of the joint was analysed in terms of the stresses that occur in the material and of the forces transmitted through the contacting surfaces. The Ansys parametric design language (APDL) was used to introduce the commands for representing diagrams of stress, deformation at the joint and forces on the surfaces of each member, as well as the commands for obtaining the numerical values of forces and bending moments at the joint. Such a procedure enables the user to know the stress state obtained from a finite element model and to compare the result with the conventional theory applied to this type of joint.

The automated model was used to analyse the influence on the behaviour of the node of different geometric parameters such as the angle between intersecting members or the variation in the friction coefficient between contacting surfaces, and to analyse the effects of increasing the load at the joint.

The second step consisted in optimising the geometric characteristics defined in the Spanish Technical Building Code CTE-SE-M (2006) for framed joints. Optimisation was based on the geometric definition expressions that must be satisfied by framed joints in order to obtain structural stability (1): notch t and chord shear length a (Equations 8.79 and 8.80 of the Technical Building Code; see Fig. 2). The joint was modelled by finite elements using the dimensions that were obtained from both expressions by applying the acting forces obtained from conventional design. Then, the stress state was calculated by using the finite element method (2). After having obtained the stresses acting on the joint and, therefore, the forces acting on the contacting surfaces, the model introduced these real values internally

and checked the different sections and critical points of the joint (shear stress on the tie-end and compression oblique to the grain), giving new values of a and t (3) as output. Moreover, the model considered the possibility of reducing the dimensional requirements contained in the Spanish Technical Building Code based on the real stress conditions obtained for the joint. When such a reduction was possible, the process generated successive iterations (4) until there was agreement between the dimensions introduced in the model and the appropriate safety conditions for the critical sections, which enabled convergence to stable geometry values. As a result, the reduction factor for the original expressions could be obtained based on the availability of the real stresses that occurred at the critical sections of the joint (5).

The flow diagram of the above process is presented in Fig. 2.

Results

Numerical simulations were performed using the joints obtained from analysing the different possibilities for the trusses, which were described in the above sections. The results from numerical simulations were compared with the results that would be obtained from conventional design, and the correlations between the results obtained by using both methods were found.

As compared to conventional design, the value of F_1 decreases linearly with the increase in the angle, even exceeding 30% decrease. Conversely, F_2 shows an opposite variation. The shear stress value obtained on the tie-end decreases with the increase in the angle, ranging from slightly above 10% decrease for small angles to almost 30% decrease for 45° angles. This behaviour results from simulating friction between contacting surfaces. In such a simulation, part of the force that would act directly on the tie-end in conventional design is retained by the shear stress, mainly on the surface of F_2 .

Similarly, with the increase in the angle, the tangential component of the force increases with respect to the normal component in both contacting surfaces. The value of the shear stress in the tie-end decreases with the increase in the angle as a direct consequence of the decrease in the horizontal component of the force transmitted by the rafter.

The gradual increase in the axial forces acting on the joint causes linear increases in the stresses and the shear force acting on the tie-end. The rate or slope of the

increase is dependent on the angle between intersecting members.

The variation in the friction coefficient between contacting surfaces affects the results obtained for the values of forces transmitted at the joint. An increase in μ notably increases F_2 and decreases F_1 , mainly due to the large increase observed in the tangential component of F_2 , which is generated by friction in the large surface. The shear stress value decreases with the increase in μ , and the slope of the decrease is steeper for large angles, which is consistent with the observations made for F_1 and F_2 .

The decrease in the axial force at the notch as compared to the tie is more pronounced for larger angles, with values around 25% for angles near 45°.

With the increase in the friction coefficient, the ratio between the axial force at the notch and the axial force in the tie decreases, *i.e.* the percentage of stress in the reduced section is lower. Such a decrease with respect to μ is dependent on the skew angle between rafter and tie.

In order to modify the expression provided by CTE-(SE-M) for estimating notch t and chord shear length a , new expressions that reflect the effect of the angle and of the friction coefficient can be obtained by introducing a second cosine of the angle that includes the effect of the new stress distribution caused by the occurrence of friction at the contact between members, which was not considered in conventional design. Values a and t show a similar variation.

Stress behaviour of the joint

The next paragraphs introduce a number of figures that illustrate the behaviour of the joint from the perspective of numerical simulation and provide examples of the results at one of the joints studied.

Figure 3 shows a deformation of the joint caused by the forces transmitted by truss members.

The distribution of stresses parallel to the grain in the members intersecting at the node is represented in Figure 4, with a skew angle of connection (β) between members of 45°.

Figure 5 shows the distribution of forces along the notch at the end of the rafter and represents the stress variation along the contacting surfaces. The stresses represented in Figure 5 are within normal values, assuming an average value of yield stress in parallel compression for Scots pine of 39 N mm⁻², based on the tests conducted by Argüelles Bustillo (1994) with Scots pine specimens of Spanish origin.

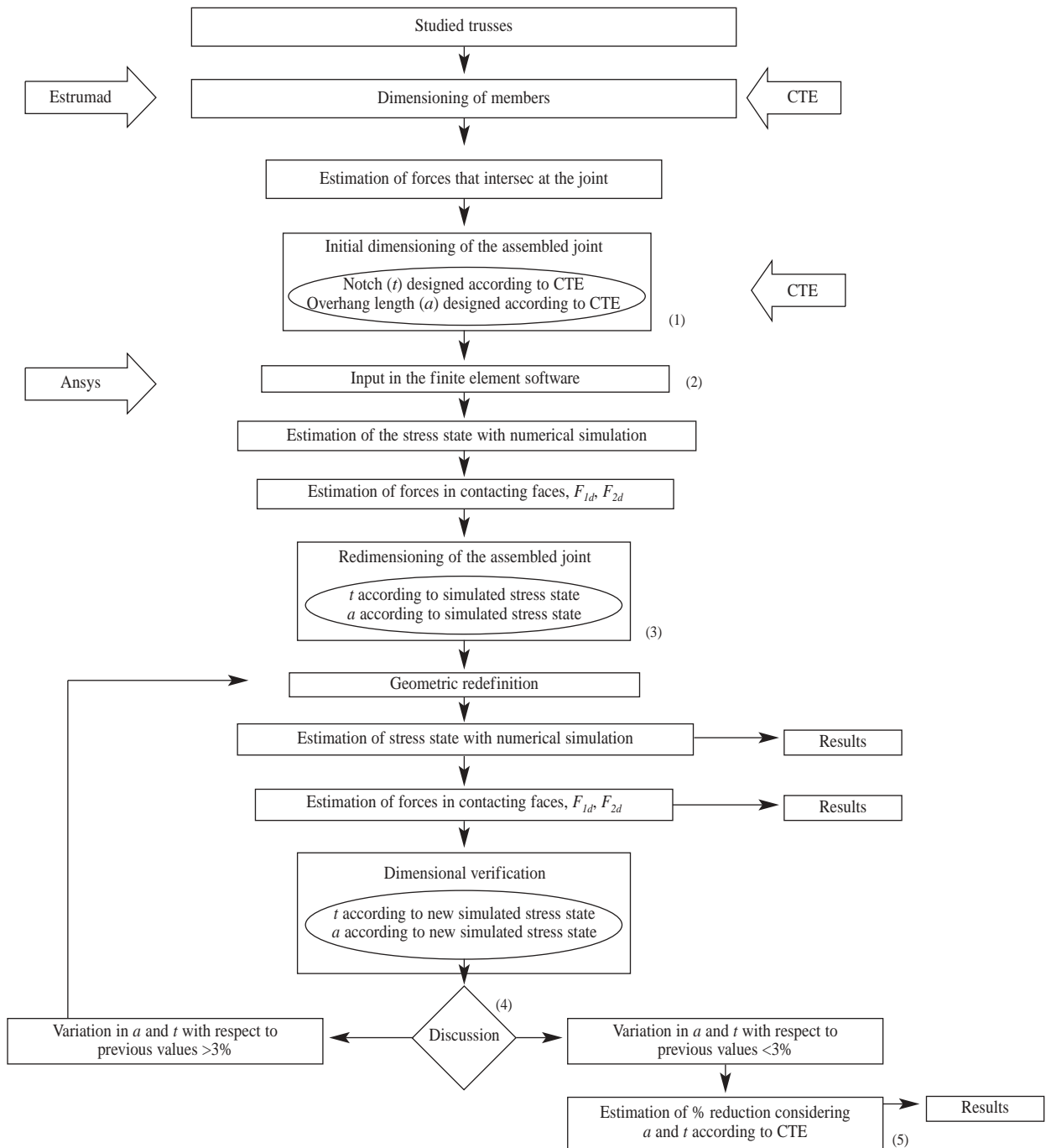


Figure 2. Flow diagram of the method used; CTE is the abbreviation for Spanish Technical Building Code CTE-SE-M (2006).

As shown in Figure 5A, the inclination of the rafter with respect to the tie produces a distribution of nodal forces in which maximum values occur at section ends. Force distribution inside the section is relatively uniform. The maximum value for small skew angles occurs only at the bottom of the small contacting sur-

face and is higher than the maximum value for larger angles. Such a result derives from the fact that almost the entire axial force transmitted by the rafter is applied on that surface. However, for larger angles, forces are distributed along the two surfaces of the joint.

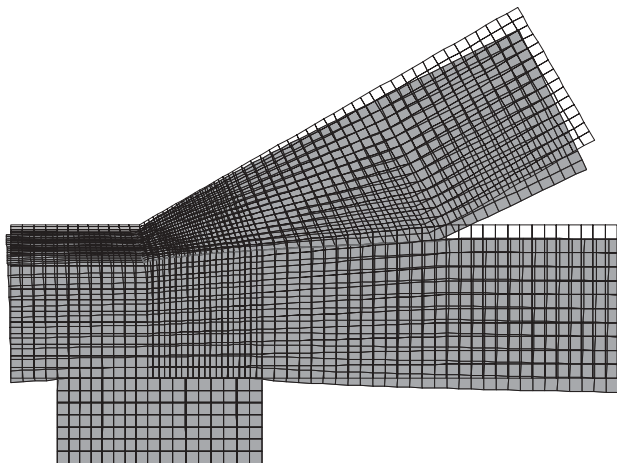


Figure 3. Deformation of the cogging joint and undeformed mesh.

Figure 5B shows the distribution of stresses along the large surface. For large angles, the large contacting surface is very important in terms of tangential and normal stresses. Conversely, stresses do not assume significant values for small angles. In such cases, the small surface receives almost the entire transmission of forces between

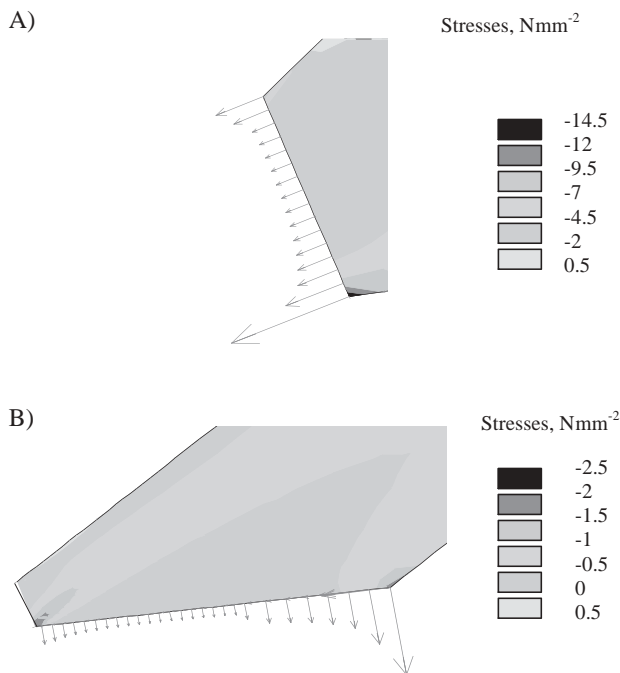


Figure 5. Representation of nodal forces. A: on the surfaces of $F_{1,d}$ and compression oblique to the grain in the rafter for an angle of 45° , N mm^{-2} . B: on the surfaces of $F_{2,d}$ and compression oblique to the grain in the rafter for an angle of 45° , N mm^{-2} .

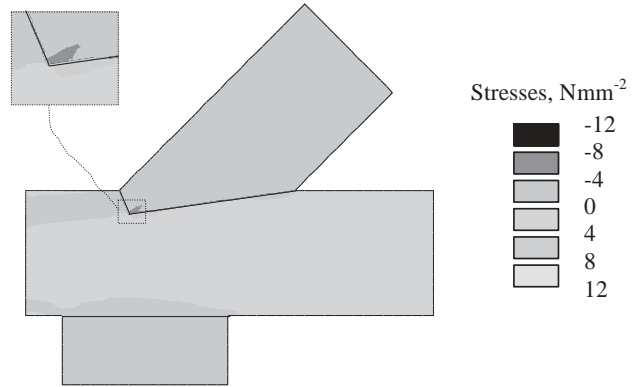


Figure 4. Normal stresses σ_x parallel to the grain in each member for an angle of 45° , N mm^{-2} .

en rafter and tie. These results suggest that the skew angle (β) between members is the parameter with the strongest influence on force and stress estimation, as shown in further sections.

Figure 6 shows the distribution and shape of shear stresses in the tie-end.

Relationship between forces obtained from simulation and forces obtained from conventional design

The analysis of the simulations performed reveals variations between the values of the forces obtained by finite element modelling and the results obtained by conventional design. This section shows different figures that represent such variations as a function of angle and timber strength class.

As compared to conventional design, the value of F_1 decreases linearly with the increase in the angle (Fig. 7A). Figure 7A represents the relationship between F_{1fem} and F_1 . The opposite behaviour is observed for F_2 (Fig. 7B). The value of the shear stress in the tie-end decreases with the increase in the angle, as

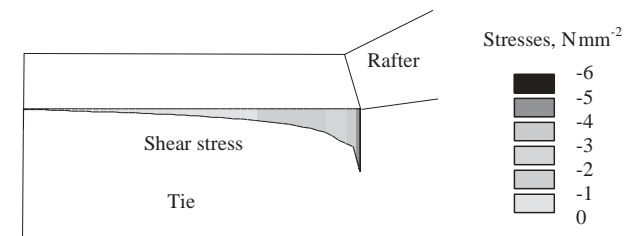


Figure 6. Shear stress in the tie-end, N mm^{-2} .

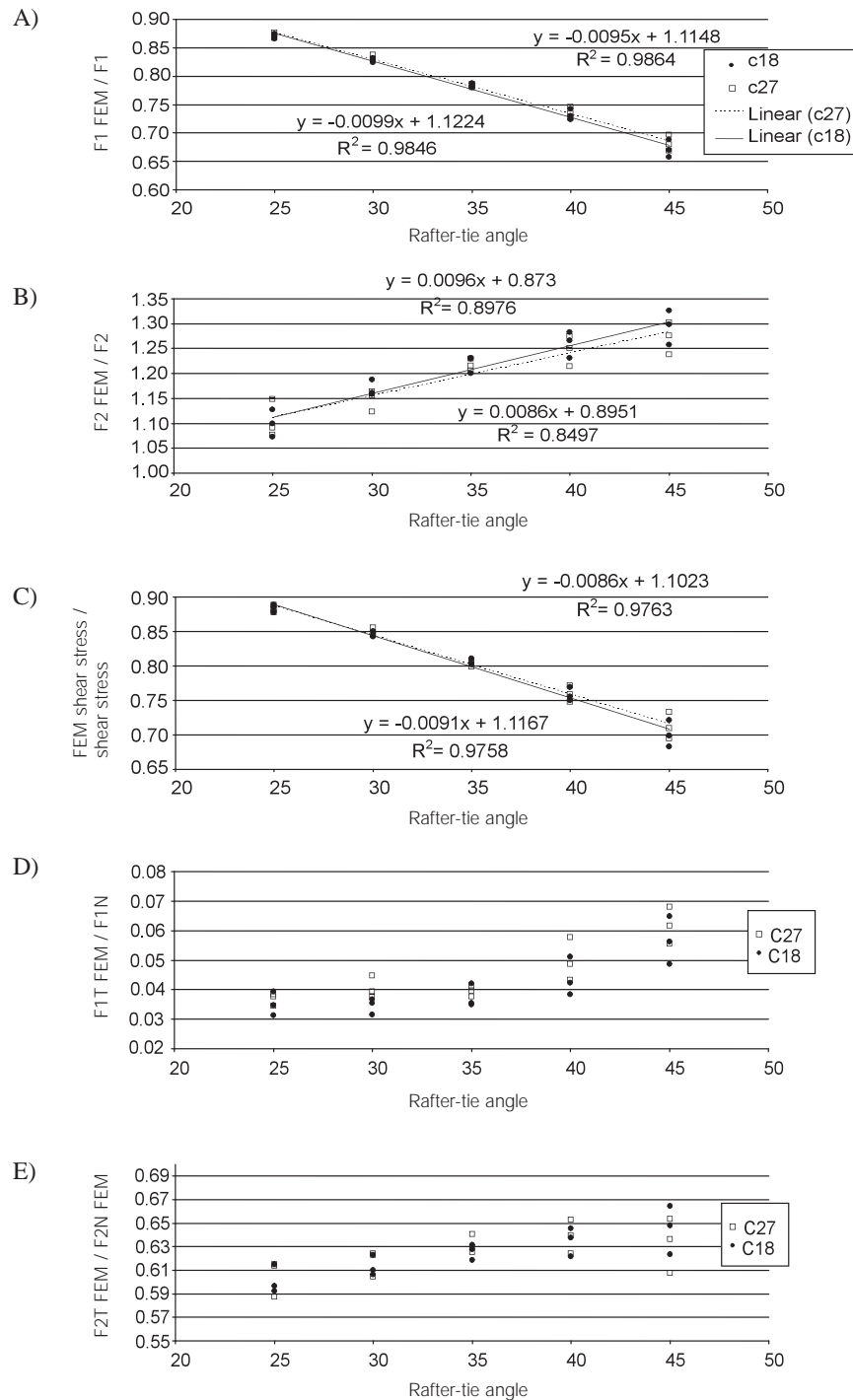


Figure 7. Relationship between finite element method (FEM) and design. A: Relationship F_1 obtained from FEM simulation (F1 FEM) and conventional design (F_1) for different angles and strength classes. B: Relationship between F_2 obtained from finite element simulation (F2 FEM) and conventional design (F_2) for different angles and strength classes. C: Relationship between the shear stress in the tie-end obtained from finite element simulation (FEM shear stress) and conventional design (shear stress) for different angles and shear stresses. D: Relationship between the tangential component (FIT FEM) and the normal component (FIN FEM) in the small surface, as obtained from finite element simulation for different angles and strength classes. E: Relationship between the tangential component (F2T FEM) and the normal component (F2N FEM) in the large surface, as obtained from finite element simulation for different angles and strength classes.

shown in Figure 7C. With the increase in the angle, the tangential component of the force increases with respect to the normal component in both contacting surfaces (Figs. 7D and 7E), yet, the linearity of these results is not as definite as in previous Figures 7A, 7B and 7C.

Relationship between the axial force transmitted by the tie and the axial force at the notch

This section studies the relationship between the axial force in a complete section of the tie and the axial force transmitted to the notch to form the traditional joint, which corresponds to the “ $h - t$ ” height shown in Fig. 1A.

The decrease in the axial force at the notch with respect to the axial force in the tie is more pronounced for large angles. This behaviour results from the larger force applied to the large surface at these angles, which causes higher friction and, consequently, higher absorption of the axial force by the horizontal component of the total force applied to the large surface. Figure 8 represents the results obtained from the numerical simulation of cogging joints in the analysed trusses as a function of the angle. The variation observed for each angle is caused by other variables.

In addition, variation can be a function of the friction coefficient, which is reasonable because friction in the large surface is an important point of absorption of the axial force, as suggested above. The ratio between the axial force at the notch and the axial force in the tie decreases, *i.e.* the percentage of stress in the reduced section becomes lower. Such a decrease with respect to μ depends on the skew angle between rafter and tie. As for other parameters, variation according to strength class is almost negligible.

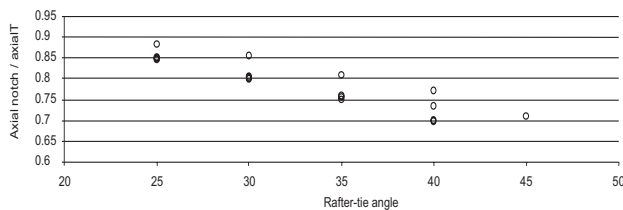


Figure 8. Relationship between the axial force at the notch and the axial force in the tie ($Axial\ notch / axialT$) for different values of the β angle between rafter and tie at the joint.

Geometric characteristics of the traditional joint as obtained from numerical simulation results

Figure 9 shows the results obtained for the geometric characteristics of the joint. The figure represents the reduction per unit of the load capacity of the joint obtained from the numerical simulation as compared to the values obtained from direct application of the expressions suggested in CTE-SE-M (2006) for the dimensional values of notch t and chord shear length a . Such a reduction is plotted against the angle formed by intersecting members at the joint, considering the friction coefficient μ used.

The values of μ assumed for discussion ranged from 0.6 for dry timber to 0.83 for green timber. With the increase in μ , F_2 increases and F_1 decreases because of the large increase in the shear component of F_2 generated by friction in the large surface.

Such a decrease in F_1 directly affects related geometric characteristics of the joint, such as the variables a and t envisaged in the Spanish Technical Code. As shown in Figure 9, these variables are also affected by linear variation.

In all cases, reduction per unit decreases with the increase in the cosine of the angle (decrease in the angle). Such a decrease converges practically in all cases for a value of 0.1, but the slope of the decrease differs according to the coefficient, being steeper for a

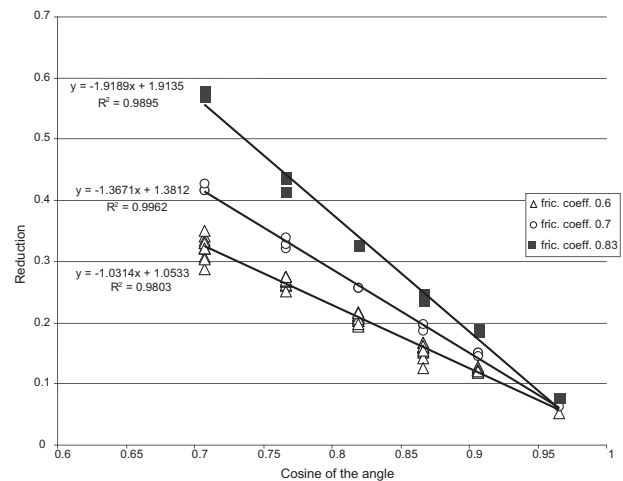


Figure 9. Reduction per unit in chord shear length a and notch t dimensions as a function of the angle between the members of the joint and of the friction coefficient between contacting surfaces.

coefficient of 0.83 and milder for 0.6, which suggests that the decrease is more pronounced for cosines of angles of 45 degrees, becoming even more pronounced with the increase in the friction coefficient. Strength class does not have any effect on these results.

The expressions for each value of the friction coefficient were obtained by regression from this graph as a function of the cosine of the angle. The following expressions were obtained by applying regressions to the expression contained in the CTE-(SE-M) for obtaining a "corrected" value of a and t that considered the corresponding reduction (value of y in the Figure 9):

$$a \geq \frac{F_d \cdot \cos \beta}{b \cdot f_{v,d}} \cdot (1-y) \quad t \geq \frac{F_d \cdot \cos \beta}{b \cdot f_{c,\alpha,d}} \cdot (1-y)$$

The following expressions are obtained by introducing the regressions obtained and applying them to chord shear length a :

For $\mu=0.6$:

$$a \geq \frac{F_d \cdot \cos \beta}{b \cdot f_{v,d}} \cdot (1.0314 \cos \beta - 0.0533)$$

For $\mu=0.7$:

$$a \geq \frac{F_d \cdot \cos \beta}{b \cdot f_{v,d}} \cdot (1.3670 \cos \beta - 0.3812)$$

For $\mu=0.83$:

$$a \geq \frac{F_d \cdot \cos \beta}{b \cdot f_{v,d}} \cdot (1.9189 \cos \beta - 0.9135)$$

To introduce the coefficient in the equation, the transverse variation of these equations was analysed. The variation in the coefficients of the above equations was linear, with an R^2 value close to 1, which results from the linearity of the variation in the reduction of a and t with respect to the friction coefficient. By introducing transverse variation in the equations above, the following expression is obtained:

$$a \geq \frac{F_d \cdot \cos \beta}{b \cdot f_{v,d}} \cdot [(3.8776\mu - 1.3140) \cos \beta - (3.7573\mu - 2.2184)]$$

Simplified as:

$$a \geq \frac{F_d \cdot \cos \beta}{b \cdot f_{v,d}} \cdot k$$

$$t \geq \frac{F_d \cdot \cos \beta}{b \cdot f_{c,\alpha,d}} \cdot k$$

Where:

$$k = [(3.88\mu - 1.31) \cos \beta - (3.76\mu - 2.22)]$$

These results suggest that, in addition to the friction coefficient, a second cosine of the angle affects the expressions for the estimation of a and t . The second cosine includes the effect of stress distribution as a function of the angle formed by the members, which was not considered in the conventional design suggested in CTE-SE-M because the occurrence of friction was neglected.

The expressions provided above can be used to quantify the safety level with which the Spanish Technical Building Code CTE-SE-M (2006) designs cogging joints. These expressions suggest the percentage by which the values of a and t could be reduced while maintaining the load capacity of the joint considering the stress state obtained from finite elements as compared to the values recommended by the Spanish Technical Building Code.

Discussion

The FEM analysis of the cases studied reveals the importance of the effect of friction on the contacting surfaces, which had already been evidenced by Moses and Prion (2003) for bolted connections. The total force acting on each of the surfaces is split into a normal component and a tangential component, producing an inclination of the resultant, which becomes more efficient in the transmission of forces between members.

The skew angle formed by rafter and tie is a key factor in the distribution of stresses along the contacting surfaces between members. The value of the angle is the most important factor in the behaviour of the joint and intrinsically affects the effects of varying other parameters, as reported by Parisi and Piazza (2002). In general, strength class hardly affects the results obtained when other parameters are varied.

The stress variation along the contacting surfaces evidenced by numerical simulation deviates from conventional design assumptions of regular distributions of stresses along the contacting surfaces (Argüelles *et al.*, 2003), but such assumptions are simplifications.

The variation in the friction coefficient between contacting surfaces affects the values obtained for tangential stresses and for the forces acting on the surfaces. However, the influence of varying the friction coefficient is minimised because structural timber

should be dry; generally, green timber is not used for structures.

The value of the force applied on the small surface (F_1) decreases linearly with the increase in the skew angle, as compared to conventional design. For angles of 45°, the value of this force decreases by 30%. The force applied on the large surface (F_2) shows the opposite variation.

As compared to conventional design, the value of the shear stress in the tie-end decreases as a consequence of the occurrence of friction between contacting surfaces because the shear stress, mainly on the large contacting surface, retains part of the force that would otherwise act directly on the tie-end. Shear stress decreases linearly with the increase in the angle, exceeding 25% reduction for angles near 45°.

The decrease in the axial force observed at the notch with respect to the axial force in the tie ranges from 10% for small skew angles, of around 25°, to over 25% for large angles, of around 45°.

These results are not surprising: for small angles, almost the entire force is transmitted normally to the small surface, while an increase in the angle brings about an increase in static friction in both surfaces.

The occurrence of friction between contacting surfaces, which is not considered in the conventional design contained in the Spanish Technical Building Code CTE-SE-M (Ministerio de la Vivienda, 2006), is evidenced in this type of joint by means of a second cosine of the angle formed by the intersecting members that affects the design of the notch t , of the chord shear length a , and of the forces transmitted along each contacting surface. The variation in the reduction of a and t with respect to the friction coefficient is linear because of the linearity of the variation in the forces acting on the contacting surfaces to vary the friction coefficient.

The geometrical recommendations contained in the Spanish Technical Building Code for notch depth t and chord shear length a consider a high level of safety.

Acknowledgements

This work was funded by the Spanish government, *Plan Nacional del Ministerio de Ciencia y Tecnología*, within the framework of research project AGL2005-04418, co-funded by the European Regional Development Fund (ERDF) and by the Galician government *Xunta de Galicia*, within the framework of research project PGIDIT02RAG20905PR.

References

- ANSYS, 2003. Theory manual version 8.1. Ansys, Inc., Canonsburg, USA.
- ARGÜELLES R., ARRIAGA F., MARTÍNEZ J.J., 2003. Estructuras de madera. Diseño y Cálculo. AITIM. Asociación de Investigación Técnica de las Industrias de la Madera y Corcho, Madrid, Spain. [In Spanish].
- ARGÜELLES ÁLVAREZ R., ARGÜELLES BUSTILLO R., ARRIAGA MARTITEGUI F. 2006. Design and calculus of wood structures. ESTRUMAD, Version 2006. Bellisco Madrid, Spain.
- ARGÜELLES BUSTILLO R., 1994. Predicción con simulación animada del comportamiento de piezas de madera, PhD Thesis. ETSI de Montes, Universidad Politécnica de Madrid, Spain. [In Spanish].
- CEN, 2003. Structural timber. Strength Classes. EN 338. European Committee for Standardization, Brussels, Belgium.
- CEN, 2004a. Design of timber structures. Part 1-1. EN 1995-1-1 Eurocode 5. European Committee for Standardization, Brussels, Belgium.
- CEN, 2004b. Structural timber. Strength classes. Assignment of visual grades and species. EN 1912, European Committee for Standardization, Brussels, Belgium.
- CHEN C.J., LEE T.L., JENG D.S., 2003. Finite element modeling for the mechanical behavior of dowel-type timber joints. *Comput Struct* 81(30-31), 2731-2738. doi:10.1016/S0045-7949(03)00338-9.
- ELLEGAARD P., 2006. Finite-element modeling of timber joints with punched metal plate fasteners. *J Struct Eng* 132(3), 409-417. doi:10.1061/(ASCE)0733-9445(2006)132:3(409).
- GUPTA R., GEBREMEDHIN K.G., 1990. Destructive testing of metal-plate-connected wood truss joints. *J Struct Eng* 116(7), 1971-1982. doi:10.1061/(ASCE)0733-9445(1990)116:7(1971).
- GUPTA R., GEBREMEDHIN K.G., 1992. Resistance distributions of a metal-plate-connected wood truss. *Forest Prod J* 42(7/8), 11-16.
- GUPTA R., GEBREMEDHIN K.G., COOKE R.J., 1992. Analysis of metal-plate-connected wood trusses with semi-rigid joints. *T ASAE* 35(3), 1011-1018.
- HUSSEIN R., 2000. Parametric investigation of the buckling performance of metal-plate-connected joints. *Adv Eng Softw* 31(1), 45-56. doi:10.1016/S0965-9978(99)00032-0.
- KESSEL M.H., 1995. Computer aided design and manufacturing. Timber Engineering STEP 2-C12. Design-Details and structural systems. Centrum Hout, The Netherlands.
- KHAROUF N., MCCLUR G., SMITH I., 2003. Elastoplastic modelling of wood bolted connections. *Comput Struct* 81, 747-754. doi:10.1016/S0045-7949(02)00482-0.

- LUSAMBO E., WILLS B.M.D., 2002. The strength of wire-connected round timber joints. *Biosyst Eng* 82(3), 339-350. doi:10.1006/bioe.2002.0070.
- MINISTERIO DE LA VIVIENDA, 2006. Código técnico de la edificación. Documento básico. Seguridad estructural. Estructuras de madera. CTE-SE-M, Ministerio de la Vivienda, Madrid, Spain. [In Spanish].
- MOSES D.M., PRION H.G.L., 2003. A three-dimensional model for bolted connections in wood. *CJCE* 30(3), 555-567. doi:10.1139/103-009.
- NATTERER J., SANDOZ J.L., REY M., 2000. Construction en bois. Matériau, technologie et dimensionnement. Presses Polytechniques et Universitaires Romandes, Lausanne, Switzerland. [In French].
- PARISI M.A., PIAZZA M., 2002. Seismic behaviour and retrofitting of joints in traditional timber roof structures. *Soil Dyn Earthq Eng* 22, 1183-1191. doi:10.1016/S0267-7261(02)00146-X.
- SAWATA K., YASUMURA M., 2003. Estimation of yield and ultimate strengths of bolted timber joints by nonlinear analysis and yield theory. *J Wood Sci* 49(5), 383-391. doi:10.1007/s10086-002-0497-3.
- SIA, 2002. Projet 505 265. Constructions en bois. Ed. Société des Ingénieurs et des Architectes. Zurich, Switzerland. [In French].
- SIMO J.C., LAURSEN T.A., 1992. An augmented Lagrangian treatment of contact problems involving friction. *Comput Struct* 42(1), 97-116. doi:10.1016/0045-7949(92)90540-G.
- STEHN L., BORJES K., 2004. The influence of nail ductility on the load capacity of a glulam truss structure. *Eng Struct* 26(6), 809-816. doi:10.1016/j.engstruct.2004.01.012.
- USDA, 1974. Wood handbook: Wood as an engineering material. Forest Products Laboratory, US Department of Agriculture, Washington, DC, USA.
- VATOVEC M., GUPTA R., MILLER T.H., 1996a. Testing and evaluation of metal-plate-connected wood truss joints. *J Test Eval* 24(2), 63-72.
- VATOVEC M., MILLER T.H., GUPTA R., 1996b. Modeling of metal-plate-connected wood truss joints. *T ASAE* 39(3), 1101-1111.
- VATOVEC M., GUPTA R., MILLER T.H., LEWIS S., 1997. Modeling of metal-plate-connected wood truss joints: Part II: Application to overall truss model. *T ASAE* 40(6), 1667-1675.
- VIDAL P., GUAITA M., AYUGA F., 2005. Analysis of dynamic discharge pressures in cylindrical slender silos with a flat bottom or with a hopper: comparison with Eurocode 1. *Biosyst Eng* 91(3), 335-348. doi:10.1016/j.biosystem-seng.2005.03.012.
- WILLIAMS J.M., FRIDLEY K.J., COFER W.F., 2000. Falk failure modelling of sawn lumber with a fastener hole. *Finite Elem Anal Des* 36(1), 83-98. doi:10.1016/S0168-874X(00)00010-X.